Applied Energy 135 (2014) 634–642

Contents lists available at ScienceDirect

Applied Energy

journal homepage: www.elsevier.com/locate/apenergy

Potential for increased wind-generated electricity utilization using heat pumps in urban areas

Michael Waite *, Vijay Modi

Department of Mechanical Engineering, Columbia University, USA

HIGHLIGHTS

- Large-scale wind power and increased electric heat pumps were evaluated.
- A deterministic model of wind power and electricity demand was developed.
- Sub-models for space heating and domestic hot water demand were developed.
- Increased use of heat pumps can improve the viability of large-scale wind power.
- Larger wind power capacity can meet a target utilization rate with more heat pumps.

ARTICLE INFO

Article history:
Received 26 November 2013
Received in revised form 8 April 2014
Accepted 21 April 2014
Available online 10 May 2014

Keywords:
Renewable energy resources
Wind power
Heat pumps
Systems integration
Urban energy

ABSTRACT

The U.S. has substantial wind power potential, but given wind's intermittent availability and misalignment with electricity demand profiles, large-scale deployment of wind turbines could result in high electricity costs due to energy storage requirements or low utilization rates. While fuel switching and heat pumps have been proposed as greenhouse gas (GHG) emissions and energy reduction strategies at the building scale, this paper shows that heat pump adoption could have additional system-wide benefits by increasing the utilization of wind-generated electricity. A model was developed to evaluate the effects of coupling large-scale wind power installations in New York State with increased use of electric heat pumps to meet a portion of space heating and domestic hot water (DHW) demands in New York City. The analysis showed significant increases in wind-generated electricity utilization with increased use of heat pumps, allowing for higher installed capacity of wind power. One scenario indicates that 78.5% annual wind-generated electricity utilization can be achieved with 3 GW of installed wind power capacity generated electricity equal to 20% of existing NYC annual electricity demand; if 20% of space heating and DHW demands are provided by heat pumps, the 78.5% utilization rate can be achieved with an increase of total wind power capacity to 5 GW. Therefore, this integrated supply–demand approach could provide additional system-wide emissions reductions.

1. Introduction

Dense urban areas are often considered energy efficient because individuals tend to use less energy than residents of suburban and rural areas [1]. However, the cumulative effect in New York City (NYC) and other urban areas is a large, concentrated energy demand. The potential for in-zone renewable energy is limited in urban areas due to high energy demands relative to geographical size and land area; shading and microclimate effects from buildings and infrastructure; and limited space for equipment installations. NYC is projected to require 33% of the total annual electricity demand (excluding transportation) for New York State (NYS) in 2022 with NYC renewable energy resources representing only 16% of the statewide technical potential and only 2.2% of what is deemed economically viable statewide [2]. Therefore, integration of renewable energy into the larger electricity grid serving NYC will be required to offset urban fossil fuel usage.

Renewable energy resources, such as wind and solar, are intermittent: supply profiles do not necessarily align with demand profiles. As such, the need for energy storage to increase the utilization of electricity generated has been widely accepted [3]. This can be costly and render large-scale renewable energy deployments infeasible [4]. Further, these considerations ignore the dominant energy

* Corresponding author. Address: Mechanical Engineering Department, Columbia University, 220 S.W. Mudd Building, 500 West 120th Street, New York, NY 10027, USA. Tel.: +1 212 854 7993.

E-mail address: mbw2113@columbia.edu (M. Waite).

http://dx.doi.org/10.1016/j.apenergy.2014.04.059
0306-2619/

Nomenclature

A total NYC floor area for a particular building type (m^2)
COP_{DHW} domestic hot water heat pump coefficient of performance
COP_{SH} space heating heat pump coefficient of performance
D_{base} base electricity demand (MW h)
D_{EOB} existing electricity demand over base load (MW h)
D_{DHW} electricity demand for additional DHW heat pumps (MW h)
D_{NYC} New York City electricity demand (MW h)
D_{SH} electricity demand for additional SH heat pumps (MW h)
E_{grid} existing grid electricity utilized to meet demands (MWh)
$E_{grid,DHW}$ existing grid electricity utilized for DHW through additional electric heat pumps (MW h)
$E_{grid,EOB}$ existing grid electricity utilized for existing electricity demand over base load (MW h)
E_{gridSH} existing grid electricity utilized for SH through additional electric heat pumps (MW h)
$E_{gridtot}$ total annual grid electricity utilized to meet demands (MWh)
E_{wind} wind-generated electricity utilized to meet demands (MW h)
$E_{windDHW}$ wind-generated electricity utilized for DHW through additional electric heat pumps (MW h)
$E_{windEOB}$ wind-generated electricity utilized for existing electricity demand over base load (MWh)
E_{windSH} wind-generated electricity utilized for SH through additional electric heat pumps (MW h)
$E_{windtot}$ total annual wind-generated electricity utilized to meet demands (MWh)
EHP_{SH} electric power draw of space heating heat pump (kW)
$ESUP_{SH}$ electric power draw of supplemental space heating (kW)
e_{total} total annual carbon dioxide equivalent emissions from building electricity and heating fuels (kg CO2e)
F_{tot} total annual heating fuel usage (MWh)
f_{DHW} fraction of total fuel usage attributed to DHW
f_{SH} fraction of total fuel usage attributed to SH
G_{wind} wind-generated electricity summed across all sites (MW h)
$G_{windtot}$ total annual wind-generated electricity (MW h)
g_{wind} electricity generated per wind turbine (MW h)
H_{DHW} domestic hot water demand (MW h)
H_{SH} space heating demand (MW h)
HD heating degrees under an 18 °C basis (°C)
HHP_{SH} heating capacity of space heating heat pump (kW)
$HSUP_{SH}$ heating capacity of supplemental space heating (kW)
N total number of wind turbines
n number of turbines at an individual site
n_{max} maximum number of turbines allowed at an individual site
p_{DHW} penetration of domestic hot water heat pumps as a percentage of the total space heating demand currently from fossil fuels
p_{SH} penetration of space heating heat pumps as a percentage of the total space heating demand currently from fossil fuels
RHP_{SH} rated nominal heating capacity of space heating heat pump (kW)
r_{fuel} GHG emissions rate for in-building fossil fuel combustion (kg CO2e/MW h)
r_{grid} GHG emissions rate for existing electricity grid (kg CO2e/MWh)
T outdoor air temperature
T_{design} space heating heat pump exterior design temperature (°C)
U_{wind} wind-generated electricity utilization (%)
η_{DHW} thermal efficiency of existing fossil fuel-burning domestic hot water equipment
η_{SH} thermal efficiency of existing fossil fuel-burning space heating equipment
η_{SUP} thermal efficiency of supplemental space heating
$\mathbf{\Phi}_{DHW}$ total annual domestic hot water fuel demand (MW h)
φ_{DHW} DHW fuel demand of a DOE Commercial Reference Building model
$\mathbf{\Phi}_{SH}$ total annual space heating fuel demand (MW h)
$\mathbf{\Phi}_{total}$ total annual fuel demand (MW h)

Subscripts
h hour of simulation
i index of wind power site
j index of building type

demands in many cities: Space heating (SH) and domestic hot water (DHW), particularly in residential buildings, which typically depend on natural gas and other fossil fuels. The use of heat pumps to meet significant greenhouse gas (GHG) emission reduction targets is typically recognized in broad renewable energy policy studies – including global [5], regional [6] and local [7] – but where the potential effects on the overall feasibility of such integrated approaches have been investigated, the curtailment of wind-generated electricity that occurs when large scale deployments are added to an existing grid have not been realistically predicted [8]. Metrics have been developed to evaluate the changes to the alignment of supply and demand profiles with intermittent resources, distributed generation and heat pumps [9], but the resulting effects on wind-generated electricity utilization at different levels of technology penetration warrant investigation. Further, the performance of heat pumps, particularly air-source heat pumps, is highly sensitive to exterior conditions [10]. Analyzing these effects requires a temporal analysis that incorporates weather data.

Strategies to better align supply and demand profiles and to reduce the need for additional storage are desired. The annual heating demand profile better aligns with the wind-generated electricity profile than does the electricity demand profile. At the individual household level, better correlation has previously been identified between wind availability and heating demands than between wind availability and electricity demands; this supports the viability of a distributed system for individual households that combined a wind turbine with a ground-source heat pump (GSHP) [11]. Due to the limited in-zone renewable energy potential in urban areas, this solution is likely limited to rural applications. However, control strategies have been identified to integrate utility-scale wind turbine deployments and electric heating loads into electricity grids for both frequency control [12] and demand response [13].

This paper discusses the analysis of approaches to shift heating demands from on-site fossil fuel to electricity to improve the utilization of utility scale wind power, reduce the cost of wind-generated electricity and reduce overall system GHG emissions. The implications of adding utility-scale wind-generated electricity to existing electricity grids [14] and broad potential for demand-side implications [15] have also been evaluated separately. The use of large-scale heat pumps for district heat applications has also been analyzed [16].

The aim of the research presented in this paper is to evaluate the effects of coupling large-scale wind power installations with increased use of electric heat pumps to meet a portion of SH and DHW demands.

2. Methodology

A deterministic model was developed in Matlab [17] to perform an hourly analysis of electricity supply and demands for various levels of wind turbine deployment and heat pump penetration. The hourly energy demands of NYC, the performance of wind turbines, and the effects of increased use of electric heat pumps on wind-generated electricity were simulated. The model was analyzed for scenarios in which only SH heat pumps were included, in which only DHW heat pumps were included, and in which a combination of heat pumps for SH and heat pumps for DHW were evaluated. Wind-generated electricity was simulated as being available to meet three distinct electricity end use demands: Existing electricity demand over base load (D_{EOB}), electricity demand for additional SH heat pumps (D_{SH}) and electricity demand for additional DHW heat pumps (D_{DHW}). The hourly wind-generated electricity utilized ($E_{wind,h}$) is given by the sum of the wind-generated electricity utilized for each of these end uses at each hour, h:

$$E_{wind,h} = E_{wind,EOB,h} + E_{wind,SH,h} + E_{wind,DHW,h} \quad (1)$$

$E_{wind,EOB,h}$: hourly wind-generated electricity utilized for existing electricity demand over base load (MW h).
$E_{wind,SH,h}$: hourly wind-generated electricity utilized for SH through additional electric heat pumps (MW h).
$E_{wind,DHW,h}$: hourly wind-generated electricity utilized for DHW through additional electric heat pumps (MW h).

At each hour, any electricity demand not met by wind-generated electricity is met by the existing electricity grid:

$$E_{grid,h} = D_{base} + E_{grid,EOB,h} + E_{grid,SH,h} + E_{grid,DHW,h} \quad (2)$$

$E_{grid,h}$: hourly existing grid electricity utilized to meet electricity demands (MW h).
D_{base}: base electricity demand (MW h).
$E_{grid,EOB,h}$: hourly existing grid electricity utilized for existing electricity demand over base load (MW h).
$E_{grid,SH,h}$: hourly existing grid electricity utilized for SH through additional electric heat pumps (MW h).
$E_{grid,DHW,h}$: hourly existing grid electricity utilized for DHW through additional electric heat pumps (MW h).

The constituents of $E_{wind,h}$ and $E_{grid,h}$ are described in Sections 2.2 through 2.4.

All data required for the analysis described in this paper is available for the years 2005 and 2006. We performed the analysis for both 2005 and 2006; however, the analysis using 2005 data is presented and discussed in this paper. The focus of this study was the potential changes in wind-generated electricity utilization from incorporating additional SH and DHW demands into the NYC electricity demand. The 2005 heating season was more representative of a typical year than was 2006: According to the New York State Energy Research and Development Authority (NYSERDA), a "Normal" New York City year has 4777 heating degree days (HDD); 2005 had 4707 HDD and 2006 had 3690 HDD [18]. Weather data for NYC Central Park station was used [19].

2.1. Wind-generated electricity model

The annual electricity output of wind turbines is less than the rated power output due to diurnal, seasonal and other climate effects. As such, a temporal model is needed to evaluate the impact of electricity generated from utility-scale wind turbine installations.

The performance curve of a commercially available 3 MW wind turbine [20] and a U.S. National Renewable Energy Laboratory (NREL) dataset containing 10-min interval simulated wind speeds for 66 sites in NYS during 2004–2006 [21] were used to calculate hourly electricity generated per wind turbine ($g^{(i)}_{wind,h}$ at each site, i. The NREL study also identified the maximum number of wind turbines that could be deployed at each site ($n_{max,i}$).

A linear program model was developed that, for a given total number of turbines (N), calculates the number of 3 MW wind turbines at each site (n_i) in order to maximize the total annual wind-generated electricity ($G_{wind,tot}$):

$$\max G_{wind,tot} = \sum_{i=1}^{66}\sum_{h} n_i \times g^{(i)}_{wind,h} \quad (3)$$

where n_i is the decision variable, representing the optimum distribution of a finite number of wind turbines under the constraints of the maximum number of wind turbines at each site and the total number of turbines across all sites:

$$0 \leqslant n_i \leqslant n_{max,i} \quad (4)$$

$$\sum_{i=1}^{66} n_i \leqslant N \quad (5)$$

The hourly wind-generated electricity, summed across all turbines at all sites for the given level of wind power penetration, is then calculated by:

$$G_{wind,h} = \sum_{i=1}^{66} n_i \times g^{(i)}_{wind,h} \quad (6)$$

2.2. NYC electricity demand

The annual electricity demand profile was generated from the New York Independent System Operator (NYISO) integrated real-time load data for Zone J (NYC) [22]. Fig. 1 shows the annual electricity demand profile for NYC.

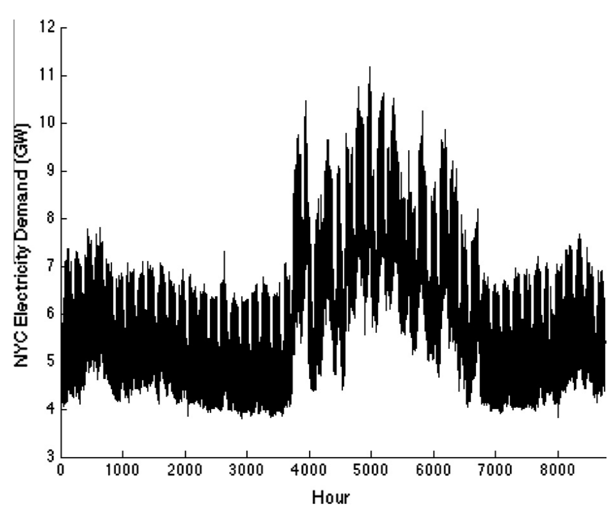

Fig. 1. Hourly electricity demand.

The NYC electricity demand at each hour ($D_{NYC,h}$) was separated into the base electricity demand (D_{base}) and electricity demand over base load ($D_{EOB,h}$):

$$D_{NYC,h} = D_{base} + D_{EOB,h} \tag{7}$$

D_{base}, assumed to be the minimum hourly demand and the same at each hour, was 3813 MW h. The peak $D_{EOB,h}$ was 7349 MW h (i.e. the peak $D_{NYC,h}$ was 11,162 MW h). Wind-generated electricity in the model first serves the hourly $D_{EOB,h}$:

$$E_{wind,EOB,h} = \begin{cases} G_{wind,h}, & G_{wind,h} \leqslant D_{EOB,h} \\ D_{EOB,h}, & G_{wind,h} > D_{EOB,h} \end{cases} \tag{8}$$

Any remaining $D_{EOB,h}$ is met by the existing electricity grid:

$$E_{grid,EOB,h} = D_{EOB,h} - E_{wind,EOB,h} \tag{9}$$

2.3. NYC heating demands

The total annual heating fuel demand ($\mathbf{\Phi}_{total}$), available from the New York City Greenhouse Gas Inventory [23], was split into total annual SH fuel demand ($\mathbf{\Phi}_{SH}$) and total annual DHW fuel demand ($\mathbf{\Phi}_{DHW}$) based on NYC fuel use splits and total floor area by building type [24]:

$$\Phi_{SH} = \frac{\sum_j f_{SH,j} \times A_j}{\sum_j A_j} \times \Phi_{total} \tag{10}$$

$$\Phi_{DHW} = \frac{\sum_j f_{DHW,j} \times A_j}{\sum_j A_j} \times \Phi_{total} \tag{11}$$

A_j: total NYC floor area for building type, j (m^2).
$f_{SH,j}$: fraction of total fuel usage attributed to SH for building type, j.
$f_{DHW,j}$: fraction of total fuel usage attributed to DHW for building type, j.

Using data from [23] and [24], $\mathbf{\Phi}_{SH}$ and $\mathbf{\Phi}_{DHW}$ were calculated to be 91.20 TW h and 23.46 TW h, respectively.

This analysis was used to investigate the effects of switching SH and DHW from on-site fossil fuels to on-site electric heat pumps powered from the grid. As such, "total annual SH demand" and "total annual DHW demand" refer only to that SH and DHW demand provided by burning fossil fuels on-site. Any existing electric heating is included in the existing electricity demand.

2.3.1. NYC space heating demand

The hourly heating degrees under an 18 °C basis (HD_h) were calculated based on hourly outdoor air temperatures for NYC (T_h):

$$HD_h = \begin{cases} 18 - T_h, & T_h < 18 \\ 0, & T_h \geqslant 18 \end{cases} \tag{12}$$

The hourly SH demand ($H_{SH,h}$) for NYC was calculated using:

$$H_{SH,h} = \eta_{SH} \times \Phi_{SH} \times \frac{HD_h}{\sum_h HD_h} \tag{13}$$

The thermal efficiency of existing fossil fuel-burning SH equipment ($\boldsymbol{\eta}_{SH}$) was assumed to correspond to the minimum performance for U.S. Environmental Protection Agency (EPA) Energy-Star-compliant equipment. An 85% SH efficiency was assumed based on the annual fuel utilization efficiency (AFUE) for a natural gas-fueled boiler [25]. The AFUE of space heating equipment is determined through laboratory tests simulating cyclic and part-load operating conditions to provide a performance metric that incorporates seasonal and operational effects [26]. Fig. 2 shows

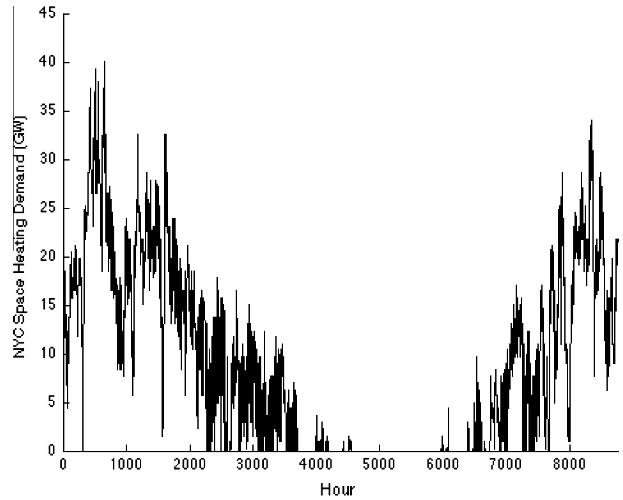

Fig. 2. Hourly space heating demand.

the hourly SH demand. The total annual SH demand was calculated to be 77.5 TW h and the peak hourly SH demand was calculated to be 40.0 GW h.

2.3.2. NYC domestic hot water demand

Eq. (14) and the hourly DHW demand profiles of the U.S. Department of Energy (DOE) Commercial Reference Buildings [27] were used to calculate the hourly DHW demand ($H_{DHW,h}$) for NYC by running the DOE-developed models in the building energy simulation tool EnergyPlus [28]. The simulation results contain the DHW fuel demand (φ_{DHW}) at each hour, h, for the building type simulated, j. The hourly DHW fuel demand was then weighted by total NYC floor area for each building type as per Eq. (14). The Reference Building models of the following building types were used: Midrise Apartment model for all NYC multifamily residential building floor area, Large Office model for all NYC office building floor area, Secondary School model for all NYC educational building floor area and Hospital model for all NYC health care facility floor area. The hourly DHW demand for 1–4 family residential buildings was assumed to scale linearly with the hourly DHW demand for multifamily residential buildings.

$$H_{DHW,h} = \eta_{DHW} \times \Phi_{DHW} \times \frac{\sum_j \varphi_{DHW,j,h} \times A_j}{\sum_h \sum_j \varphi_{DHW,j,h} \times A_j} \tag{14}$$

The thermal efficiency of existing fossil fuel-burning DHW equipment ($\boldsymbol{\eta}_{DHW}$) was assumed to be 67%, which corresponds to the minimum energy factor (EF) of EnergyStar-compliant natural gas-fueled storage water heaters [25]. EF is a measure of overall thermal efficiency of a water heater intended to reflect operational and storage effects and is determined through testing in accordance with a DOE-specified test procedure [29]. The total annual DHW demand was calculated to be 15.8 TW h and the peak hourly DHW demand was calculated to be 3.93 GW h. Fig. 3 shows the hourly DHW demand profile for a winter day (February 1st) and a summer day (August 1st). These two daily profiles are shown because the diurnal effects are difficult to discern from an annual plot; however, the figure also shows the higher DHW demand in the winter, though the seasonal differences are smaller than for the space heating demand.

2.4. Heat pump analysis

The coefficient of performance (COP) of an electric heat pump is the ratio of its heating capacity to the electricity required to operate it. The analysis discussed in this paper assumed all heat

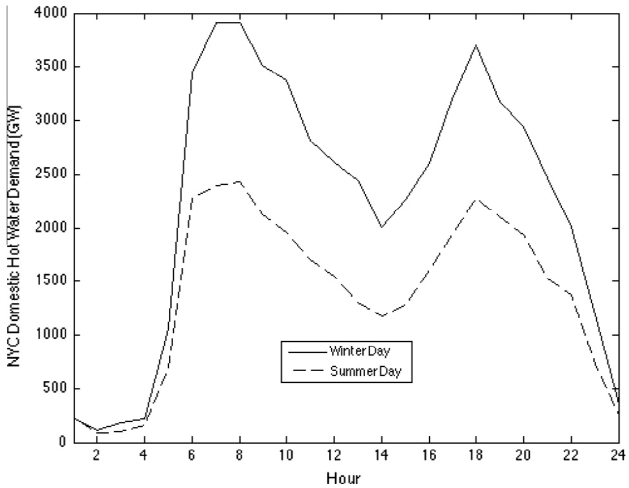

Fig. 3. Hourly DHW demand profile for winter day (February 1st) and summer day (August 1st).

pumps to be air-cooled to provide a conservative evaluation of their performance at low exterior temperatures. As such, the COP of the heat pumps in the model varied with exterior temperature.

2.4.1. Electric heat pumps for space heating

The heating capacity and electricity input of a commercially available, split-system, direct expansion (DX) electric heat pump [30] was used in the SH analysis. The electric heat pump used in the analysis is available in four sizes with rated nominal heating capacities (RHP_{SH}) of 7.03 kW, 10.6 kW, 14.1 kW and 17.6 kW. For each size, the manufacturer's published data includes the heating capacity (HHP_{SH}) and electric power draw (EHP_{SH}) of the tested system for each combination of three interior temperatures and eight exterior temperatures (T_o). To develop the exterior temperature-dependent variable COP, indoor temperatures were assumed to be 21.1 °C.

The performance data published by the manufacturer includes the effects of heating required to defrost the outdoor coil at very low ambient temperatures, but does not include any supplemental heat that may be required to meet the heating demand at these temperatures ($HSUP_{SH}$) or the electric power draw of the supplemental heat ($ESUP_{SH}$). The SH heat pump model used in this analysis includes a correction for supplemental heat that would be required at low exterior temperatures because of reduced heat pump COP and possible insufficient capacity at these temperatures. The SH heat pump COP, including the effects of supplemental heat, (COP_{SH}) for each RHP_{SH} at each T_o were determined by:

$$COP_{SH}(RHP_{SH},T_o) = \frac{HHP_{SH}(RHP_{SH},T_o) + HSUP_{SH}(RHP_{SH},T_o)}{EHP_{SH}(RHP_{SH},T_o) + ESUP_{SH}(RHP_{SH},T_o)} \quad (15)$$

For the heat pump analysis, the system was assumed to be sized using the published heating capacity for −8.3 °C exterior air (T_{design}). Supplemental electric resistance heating, with a thermal efficiency (η_{sup}) of 1, was assumed to be required below this temperature, scaling linearly with HD as per the SH demand described in Section 2.3.1:

$$HSUP_{SH}(RHP_{SH},T_o) = \begin{cases} 0, & T_o \geqslant T_{design} \\ \frac{HD(T_o)}{HD(T_{design})} \times HHP_{SH}(RHP_{SH},T_{design}) & \\ -HHP_{SH}(RHP_{SH},T_o), & T_o < T_{design} \end{cases} \quad (16)$$

$$ESUP_{SH}(RHP_{SH},T_o) = \eta_{sup} \times HSUP_{SH}(RHP_{SH},T_o) \quad (17)$$

Table 1
Space Heating Heat Pump COP.

Exterior temperature (°C)	Space heating COP
−19.4	1.27[a]
−13.9	1.57[a]
−8.3	2.42
−2.8	2.73
2.8	3.33
8.3	4.45
13.9	5.16
19.4	5.84

[a] Includes supplemental electric resistance heating.

Table 2
Domestic hot water heat pump COP.

Exterior temperature (°C)	DHW COP
<7.2	1.00[a]
7.2	1.96[b]
8	2.00
14	2.30
20	2.54
25	2.67
29.5	2.86
35	3.05
40.5	3.17

[a] Water heater operates in electric resistance heating mode.
[b] COP extrapolated from tested values at 8 °C and 14 °C.

This provides a conservative estimate of the supplemental heating required as T_{design} is lower than the typical NYC design condition and the supplemental heating model ignores the safety factors used by design engineers in sizing heating equipment.

Table 1 shows the average COP of the four heat pump sizes at each exterior temperature, calculated using Eqs. (15)–(17). The COP at each hour ($COP_{SH,h}$) was determined through linear interpolation of the values in Table 1 based on the exterior temperature (T_h) in the weather data.

For each level of SH heat pump penetration (p_{SH}) simulated, the hourly electricity demand for space heating heat pumps ($D_{SH,h}$) was calculated as:

$$D_{SH,h} = p_{SH} \times \frac{H_{SH,h}}{COP_{SH,h}} \quad (18)$$

Wind-generated electricity available after meeting the existing electricity demand is available to meet a portion of the NYC SH demand if SH heat pumps are present in the model:

$$E_{wind,SH,h} = \begin{cases} G_{wind,h} - E_{wind,EOB,h}, & G_{wind,h} - E_{wind,EOB,h} \leqslant D_{SH,h} \\ D_{SH,h}, & G_{wind,h} - E_{wind,EOB,h} > D_{SH,h} \end{cases} \quad (19)$$

Any remaining SH heat pump electricity demand is met by the existing electricity grid:

$$E_{grid,SH,h} = D_{SH,h} - E_{wind,SH,h} \quad (20)$$

2.4.2. Electric heat pumps for domestic hot water

A model of a commercially available hybrid electric heat pump storage water heater was used in the analysis. The water heater is considered a hybrid system because the water is heated by a DX heat pump at exterior temperatures of 7.2 °C or higher and by electric resistance heating at exterior temperatures below 7.2 °C. The performance characteristics of the water heater were based on laboratory testing by NREL [31]. The COP also varies with storage tank water temperature; a tank water temperature of 50 °C was assumed to assign the values in Table 2. The COP at each hour

($COP_{DHW,h}$) was determined through linear interpolation of the values in Table 2 based on the exterior temperature (T_h) in the weather data.

For each level of DHW heat pump penetration (p_{DHW}) simulated, the hourly electricity demand for space heating heat pumps ($D_{DHW,h}$) was calculated as:

$$D_{DHW,h} = p_{DHW} \times \frac{H_{DHW,h}}{COP_{DHW,h}} \tag{21}$$

Wind-generated electricity available after meeting the SH heat pump demand is available to meet a portion of the NYC DHW demand if DHW heat pumps are present in the model:

$$E_{wind,DHW,h} = \begin{cases} G_{wind,h} - (E_{wind,EOB,h} + E_{wind,SH,h}), \\ G_{wind,h} - (E_{wind,EOB,h} + E_{wind,SH,h}) \leqslant D_{DHW,h} \\ D_{DHW,h}, \\ G_{wind,h} - (E_{wind,EOB,h} + E_{wind,SH,h}) > D_{DHW,h} \end{cases} \tag{22}$$

Any remaining DHW heat pump electricity demand is met by the existing electricity grid:

$$E_{grid,DHW,h} = D_{DHW,h} - E_{wind,DHW,h} \tag{23}$$

Any excess wind-generated electricity after this step is considered not utilized or "spilled".

2.5. Wind-generated electricity utilization calculations

The primary performance characteristic calculated for each scenario was the wind-generated electricity utilization (U_{wind}): The percentage of the total annual wind-generated electricity used to meet existing electricity demand and additional SH and DHW. The total annual wind-generated electricity ($G_{wind,tot}$) and the total annual wind-generated electricity utilized ($E_{wind,tot}$) are given by the summation of the respective hourly values:

$$G_{wind,tot} = \sum_h G_{wind,h} \tag{24}$$

$$E_{wind,tot} = \sum_h E_{wind,h} \tag{25}$$

U_{wind} is given by:

$$U_{wind} = \frac{E_{wind,tot}}{G_{wind,tot}} \tag{26}$$

2.6. Emissions calculations

A full understanding of the effects of integrating new generators and demand profile changes requires a robust network model. However, for initial comparative purposes, a simplified emissions analysis was performed for each scenario analyzed.

The total annual electricity demand met by the existing grid ($E_{grid,tot}$) is given by the summation of the hourly demand met by the existing grid ($E_{grid,h}$):

$$E_{grid,tot} = \sum_h E_{grid,h} \tag{27}$$

The total annual fuel usage (F_{tot}) is given by the sum of the heating fuel usage for SH and DHW:

$$F_{tot} = (1 - p_{SH}) \times \Phi_{SH} + (1 - p_{DHW}) \times \Phi_{DHW} \tag{28}$$

The total carbon dioxide equivalent (CO2e) emissions (e_{total}) were calculated for all electricity and heating fuel (SH and DHW) demands using an average existing electricity grid GHG emissions rate (r_{grid}) and an average in-building fossil fuel combustion GHG emissions rate (r_{fuel}):

$$e_{total} = r_{grid} \times E_{grid,tot} + r_{fuel} \times F_{tot} \tag{29}$$

The average emissions rate for the 2010 electricity grid serving New York City was used for r_{grid}: 316.11 kg CO2e/MW h [23]. A weighted average fossil fuel emissions rate, based on the 2010 NYC fossil fuel usage [23], was used for r_{fuel}: 206.52 kg CO2e/MW h. (r_{fuel} is given per MW h for consistency with electricity units. In more common units for fuel-related emissions, this equates to 57.367 kg CO2e/GJ.)

3. Results and discussion

The analysis described above was performed for various levels of installed wind power capacity and penetrations of electric heat pumps replacing fossil fuels. Heat pumps were simulated for SH alone, for DHW alone and for both SH and DHW.

3.1. Wind-generated electricity

Fig. 4 shows the total annual wind-generated electricity ($G_{wind,tot}$) and capacity factor (CF) for total wind power capacity up to 17.0 GW. This wind power capacity produces a $G_{wind,tot}$, equal to the total annual NYC electricity demand. The CF is the ratio of the total annual wind-generated electricity to the maximum electricity that would be generated if the turbines operated at maximum capacity at all times.

As the total wind turbine capacity increases, the CF of the wind turbine network decreases and the relationship between installed capacity and annual output is not linear. This is due to the optimization analysis first placing wind turbines at the sites with the highest annual per turbine wind-generated electricity potential, and as an increasing number of turbines are required, placing wind turbines at sites with lower wind speeds. Therefore, as the number of wind turbines increases, the average annual wind-generated electricity per turbine decreases.

3.2. Existing electricity demand

The existing electricity demand met by wind-generated electricity in this analytical approach is independent of electric heat pump penetration. Fig. 5 shows the wind-generated electricity utilization rate, U_{wind}, versus $G_{wind,tot}$. (Note that the top x-axis does not scale linearly with the bottom x-axis per the relationship shown in Fig. 4.)

U_{wind} in the analysis decreases with increasing wind power capacity. The effect in actual installations would be lower

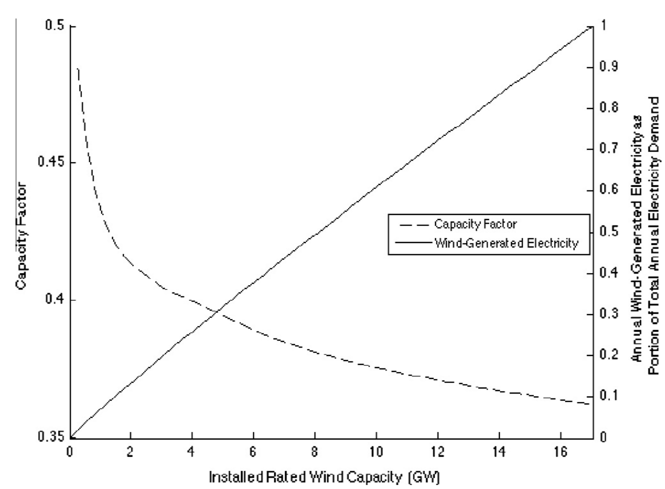

Fig. 4. Wind-generated electricity.

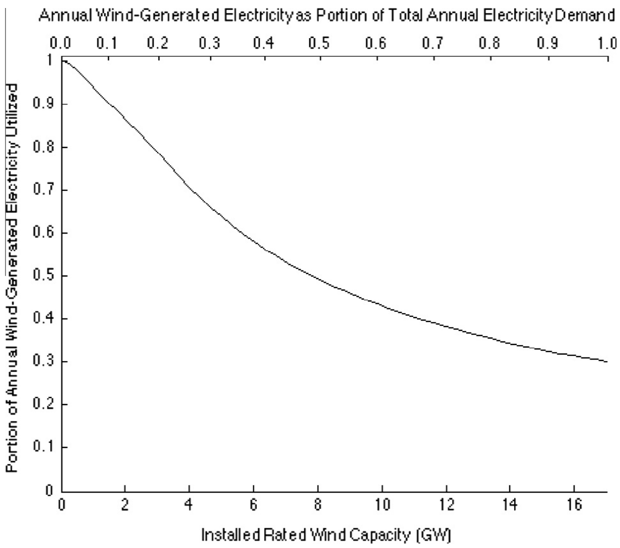

Fig. 5. Wind-generated electricity utilization to meet electricity demand over base load vs. total rated wind power capacity.

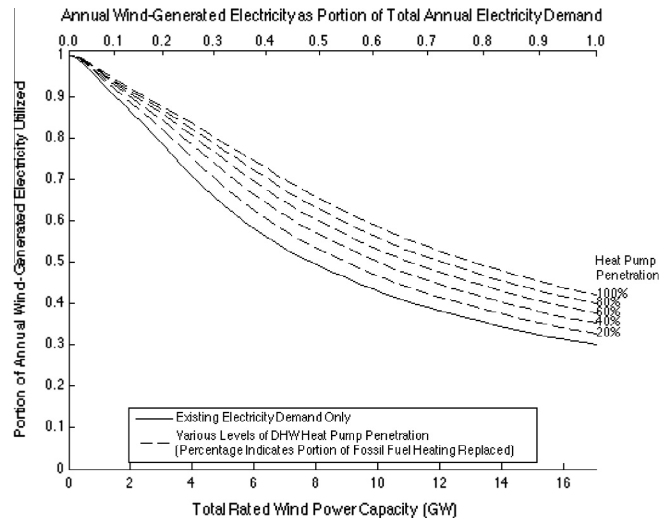

Fig. 7. Wind-generated electricity utilization to meet electricity demand over base load and various levels of DHW demand using electric heat pumps.

system-wide GHG emissions reductions without the use of energy storage. The cost of dedicated energy storage systems or the excess electricity generation implied by the results shown in Fig. 5 would result in higher per unit wind-generated electricity costs than if all wind-generated electricity could be used to meet existing electricity demands.

3.3. Electric heat pump simulations

Fig. 6 shows U_{wind} versus $G_{wind,tot}$ for various levels of SH heat pump penetration (p_{SH}).

Replacing fossil fuel-burning SH systems in the model with electric heat pumps significantly increases the wind-generated electricity utilization rate. For example, if sufficient wind power capacity (3.05 GW capacity) were installed to generate electricity equivalent to 20% of the annual NYC electricity demand, the analysis indicates that U_{wind} would increase from 78.5% under the base scenario to 88.3% if p_{SH} equaled 20%. Rather than evaluating an increase in utilization rate at a specific wind power capacity, potential investors or policymakers may set a target utilization rate in evaluating the economics of a project or policy. If the 78.5% utilization rate of the previous example was targeted and p_{SH} equaled 20%, the analysis indicates that total wind power capacity could be increased from 3.05 GW to 4.54 GW.

Fig. 7 shows U_{wind} versus $G_{wind,tot}$ for various levels of DHW heat pump penetration (p_{DHW}).

If sufficient wind power capacity (3.05 GW capacity) were installed to generate electricity equivalent to 20% of the annual NYC electricity demand, the analysis indicates that U_{wind} would increase from 78.5% under the base scenario to 81.9% if p_{DHW} equaled 20%. If a 78.5% utilization rate was targeted and p_{DHW} equaled 20%, the analysis indicates that total wind power capacity could be increased from 3.05 GW to 3.54 GW.

Although the DHW demand is significantly less than the SH demand, increases in total DHW heat pump capacity can improve the viability of large-scale wind power deployment. More moderate annual fluctuations in DHW demand, compared to the SH

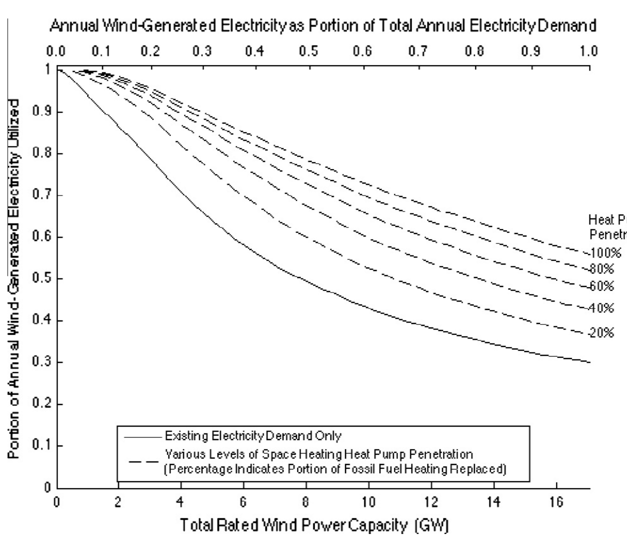

Fig. 6. Wind-generated electricity utilization to meet electricity demand over base load and various levels of space heating demand using electric heat pumps.

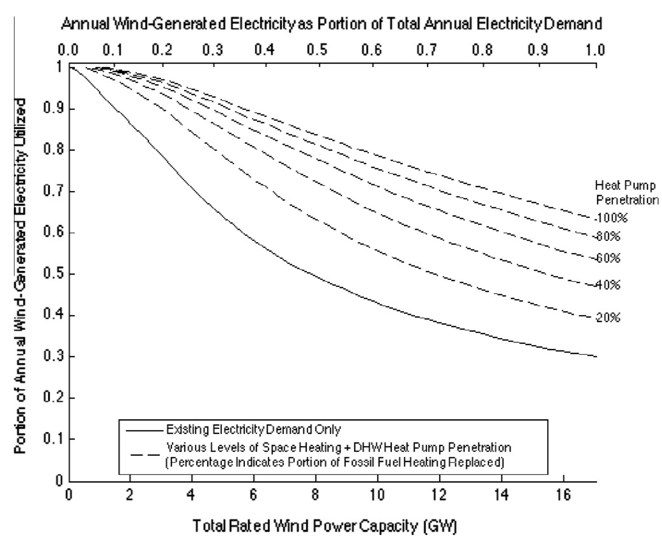

Fig. 8. Wind-generated electricity utilization to meet electricity demand over base load and various levels of space heating and DHW demand using electric heat pumps.

Table 3
Selected scenarios with total wind-generated electricity equivalent to 20% of annual NYC electricity demand.

Scenario	Percentage of wind-generated electricity utilized for following demands:				Percentage of following demands met by wind power:			Total rated wind power capacity (GW)	Emissions reduction[e] (%)
	Existing electricity (%)	Space heating	DHW	Total (%)	Existing electricity (%)	Space heating	DHW		
Base Scenario[a]	78.5	N/A	N/A	78.5	15.7	N/A	N/A	3.05	6.6
20% HPs: space heat[b]	78.5	9.8%	N/A	88.3	15.7	5.02%	N/A	3.05	13.0
20% HPs: DHW[c]	78.5	N/A	3.5%	81.9	15.7	N/A	3.54%	3.05	7.5
20% HPs: space heat+ DHW[d]	78.5	9.8%	1.6%	89.9	15.7	5.02%	1.99%	3.05	13.9

[a] Wind-generated electricity serves existing electricity demand only; no additional SH or DHW heat pumps.
[b] 20% of existing fossil fuel space heating replaced with electric heat pumps; no additional DHW heat pumps.
[c] 20% of existing fossil fuel DHW capacity replaced with electric heat pumps; no additional SH heat pumps.
[d] 20% of existing fossil fuel-burning space heating and DHW capacity replaced with electric heat pumps.
[e] Total electricity and heating fuel emissions reduction relative to case with no wind power or heat pumps.

Table 4
Selected Scenarios With 78.5% Wind-Generate Electricity Utilization Target.

Scenario	Percentage of wind-generated electricity utilized for following demands:				Percentage of following demands met by wind power:			Total rated wind power capacity (GW)	Emissions reduction[e] (%)
	Existing electricity (%)	Space heating	DHW	Total (%)	Existing electricity (%)	Space heating	DHW		
Base scenario[a]	78.5	N/A	N/A	78.5	15.7	N/A	N/A	3.05	6.6
20% HPs: space heat[b]	66.8	11.7%	N/A	78.5	19.5	8.36%	N/A	4.54	15.2
20% HPs: DHW[c]	74.5	N/A	4.0%	78.5	17.2	N/A	4.63%	3.54	8.1
20% HPs: space heat + DHW[d]	63.8	11.9%	2.8%	78.5	20.4	9.15%	4.86%	4.99	16.6

[a] Wind-generated electricity serves existing electricity demand only; no additional SH or DHW heat pumps.
[b] 20% of existing fossil fuel space heating replaced with electric heat pumps; no additional DHW heat pumps.
[c] 20% of existing fossil fuel DHW capacity replaced with electric heat pumps; no additional SH heat pumps.
[d] 20% of existing fossil fuel-burning space heating and DHW capacity replaced with electric heat pumps.
[e] Total electricity and heating fuel emissions reduction relative to case with no wind power or heat pumps.

demand, may provide a more consistent use for wind-generated electricity. Fig. 8 shows the effects of simulating both SH and DHW heat pumps.

If sufficient wind power capacity (3.05 GW capacity) were installed to generate electricity equivalent to 20% of the annual NYC electricity demand, the analysis indicates that U_{wind} would increase from 78.5% under the base scenario to 89.9% if both p_{SH} and p_{DHW} equaled 20%. If a 78.5% utilization rate was targeted and both p_{SH} and p_{DHW} equaled 20%, the analysis indicates that total wind power capacity could be increased from 3.05 GW to 4.99 GW.

3.4. Case comparison and emissions reduction

Table 3 summarizes pertinent results for scenarios in which sufficient wind power capacity (3.05 GW capacity) is installed to generate electricity equivalent to 20% of the annual NYC electric demand.

Because of the high emissions associated with burning fossil fuels on-site for SH, a relatively small portion of the heating demand met by wind can result in significant emissions reductions. This is due to two effects: (1) Wind-generated electricity being used by the heat pumps and (2) the lower emissions due to a switch from on-site fossil fuel combustion with an electric heat pump connected to the electricity grid, regardless of the lower grid emissions due to wind power. The lower relative reduction attributable to DHW heat pumps is likely the result of several factors, including lower COP (compared to SH heat pump COP) and the more consistent DHW demand throughout the year (compared to the SH demand that is highest during the peak wind seasons).

Table 4 summarizes pertinent results for scenarios in which the 78.5% utilization rate of the previous cases was set as a performance target. The heat pump penetration levels remain the same as those in Table 3.

Including heat pumps in the model with a target overall utilization rate allows for increased total wind power capacity. This increases the total amount of existing electricity demand met by wind-generated electricity. The increased wind power capacity allowed at the same wind-generated electricity utilization rate provides additional emissions reductions. Therefore, the results of this study indicate that increased heat pump penetration coupled with increased wind power capacity not only directly improves the emissions performance of the existing electricity grid and building heating requirements, but can have indirect system-wide benefits.

4. Conclusions

Increased use of electric heat pumps for space heating and domestic hot water can improve the viability of large-scale wind power deployments. The GHG emissions reductions associated with wind power have been well documented, and the potential for GHG emissions reductions from replacing fossil fuel-burning heating equipment with electric heat pumps have been commented on elsewhere. The research presented in this paper shows the effects of an integrated supply–demand approach and that additional system-wide benefits could be achieved by coupling large-scale wind power deployment with the use of electric heat pumps for space heating and domestic hot water.

The need for dedicated energy storage or wind-generated electricity "spilling" is reduced with increased use of electric heat pumps. By increasing the utilization of wind-generated electricity for the same scale of deployment (i.e. the same installed wind power capacity), fewer GHG-emitting resources would need to be used to meet energy demands. Therefore, increased penetration of electric heat pumps may reduce system-wide emissions more significantly than previously considered.

The cost of wind-generated electricity is dominated by capital costs, and the per unit cost of wind-generated electricity is dependent on the utilized portion of electricity generated: An increase in wind-generated electricity utilization decreases the per unit cost of wind-generated electricity. As such, the increased penetration of electric heat pumps may reduce the cost of wind-generated electricity.

In the event a policy or project evaluation has a specific target wind-generated electricity utilization rate, the use of electric heat pumps may significantly increase the wind power capacity that can be installed at the target utilization rate. Coupling the increased use of electric heat pumps with wind power under this scenario can provide additional system-wide emissions reductions.

Acknowledgements

Partial support for this research was provided by the National Science Foundation (NSF) IGERT "Solving Urbanization Challenges by Design" at Columbia University (NSF Award Number 0903597).

References

[1] Dodman D. Blaming cities for climate change? An analysis of urban greenhouse gas emissions inventories. Environ Urban 1999;21(1):185–201.
[2] Plunkett J, Mosenthal P, Nadel S, Elliott RN, Hill D, Neme C, Donovan C. Energy efficiency and renewable energy resource development potential in New York State, Technical Report Analysis Approach and Consolidated Results. vol. 2. New York State Research and Development Authority, Albany, New York, USA, 2003.
[3] Turner JA. A realizable renewable energy future. Science 1999;285:687–9.
[4] Hittinger E, Whitacre JF, Apt J. What properties of grid energy storage are most valuable? J Power Sources 2012;206:436–49.
[5] Jacobson MZ, Delucchi MA. Providing all global energy with wind, water and solar power, Part I: technologies, energy resources, quantities and areas of infrastructure, and materials. Energy Policy 2011;39:1154–69.
[6] Jacobson MZ, Howarth RW, Delucchi MA, Scobie SR, Barth JM, Dvorak MJ, et al. Examining the feasibility of converting New York State's all-purpose energy infrastructure to one using wind, water and sunlight. Energy Policy 2013;57:585–601.
[7] City of New York, New York City's Pathways to Deep Carbon Reductions, December 2013. Mayor's Office of Long-Term Planning and Sustainability, New York, New York, USA, 2013.
[8] Meibom P, Kiviluoma J, Barth R, Brand H, Weber C, Larsen HV. Value of electric heat boilers and heat pumps for wind power integration. Wind Energy 2007;10:321–37.
[9] Blarke MB. Towards an intermittency-friendly energy system: comparing electric boilers and heat pumps in distributed cogeneration. Appl Energy 2012;91:349–65.
[10] Lohani SP, Schmidt D. Comparison of energy and exergy analysis of fossil plant, ground and air source heat pump building heating system. Renew Energy 2010;35(6):1275–82.
[11] Kilkis IB. Utilization of wind energy in space heating and cooling with hybrid HVAC systems and heat pumps. Energy Build 1999;30:147–53.
[12] Vachirasricirikul S, Ngamroo I. Robust controller design of heat pump and plug-in hybrid electric vehicle for frequency control in a smart microgrid based on specified-structure mixed H_2/H_∞ control technique. Appl Energy 2011;88:3860–8.
[13] Broeer T, Fuller J, Tuffner F, Chassin D, Djilali N. Modeling framework and validation of a smart grid and demand response system for wind power integration. Appl Energy 2014;113:199–207.
[14] Lund H. Large-scale integration of wind power into different energy systems. Energy 2005;30:2402–12.
[15] Moura PS, de Almeida AT. The role of demand-side management in the grid integration of wind power. Appl Energy 2010;87(8):2581–8.
[16] Lund H, Möller B, Mathiesen BV, Dyrelund A. The role of district heating in future renewable energy systems. Energy 2010;35:1381–90.
[17] MATLAB, version 7.12.0 (R2011a). Natick, Massachusetts, USA: The MathWorks Inc., 2011.
[18] New York State Research and Development Authority (NYSERDA). Monthly Cooling and Heating Degree Data. (https://www.nyserda.ny.gov/Energy-Data-and-Prices-Planning-and-Policy/Energy-Prices-Data-and-Reports/Energy-Statistics-and-Weather-Data/Weather-Data/Monthly-Cooling-and-Heating-Degree-Day-Data.aspx.) Accessed April 2, 2014.
[19] United States National Oceanic and Atmospheric Administraiton National Climatic Data Center Climate Data Online (http://www.ncdc.noaa.gov/cdo-web/).
[20] Enercon. Enercon Wind Energy Converters: Product Overview, Aurich, Germany, 2010.
[21] United States National Renewable Energy Laboratory (NREL) EWITS Eastern Wind Data Set (http://www.nrel.gov/electricity/transmission/eastern_wind_dataset.html). Accessed January 30, 2012.
[22] New York Independent Systems (NYISO) (http://www.nyiso.com/).
[23] City of New York, Inventory of New York City Greenhouse Gas Emissions, September 2011, by Jonathan Dickinson and Andrea Tenorio. Mayor's Office of Long-Term Planning and Sustainability, New York, New York, USA, 2011.
[24] Howard B, Parshall L, Thompson J, Hammer S, Dickinson J, Modi V. Spatial distribution of urban building energy consumption by end use. Energy Build 2012;45:141–51.
[25] United States Environmental Protection Agency (EPA) EnergyStar (www.energystar.gov).
[26] American Society of Heating, Refrigerating and Air-Conditioning Engineers (ASHRAE). ANSI/ASHRAE Standard 103–2007: Method of Testing for Annual Fuel Utilization Efficiency of Residential Central Furnaces and Boilers, Atlanta, Georgia, USA. 2007.
[27] United States Department of Energy (DOE) Commercial Reference Building Models – New Construction (http://www1.eere.energy.gov/buildings/commercial/ref_buildings.html).
[28] United States Department of Energy. EnergyPlus Energy Simulation Software, Version 7.2. (http://apps1.eere.energy.gov/buildings/energyplus/).
[29] 10 Code of Federal Regulations (C.F.R.) 430, Subpart B, Appendix E. Washington, DC, USA, 2012.
[30] Carrier Corp. Carrier Infinity with Greenspeed; Catalog No: 25VNA-01PD. Indianapolis, Indiana, USA, 2011.
[31] Sparn B, Hudon K, Christensen D. NREL/TP-5500-52635: laboratory performance evaluation of residential integrated heat pump water heaters. Golden, Colorado, USA: NREL; 2011.